Mn-induced surface reconstructions on GaAs(001)

Akihiro Ohtake,*,† Atsushi Hagiwara,‡ Kazuya Okukita,‡ Kenta Funatsuki,‡ and Jun Nakamura‡

National Institute for Materials Science (NIMS), Tsukuba 305-0044, Japan, and Department of Engineering Science, The University of Electro-Communications (UEC-Tokyo), Chofu, Tokyo 182-8585, Japan

E-mail: OHTAKE.Akihiro@nims.go.jp

Phone: +81 (0)29 860 4198. Fax: +81 (0)29 860 4753

*To whom correspondence should be addressed
†National Institute for Materials Science
‡The University of Electro-Communications

Abstract

We have systematically studied the surface reconstructions induced by the adsoprtion of Mn atoms on GaAs(001). Several types of adsorption structures were observed depending on the preparation conditions, and were identified using complementary experimental techniques of reflection high-energy electron diffraction, scanning tunneling microscopy, reflectance difference spectroscopy, and x-ray photoelectron spectroscopy. The sequence of surface structures as a function of As coverage was confirmed by the experiments and first-principles calculations. Under the most Ga-rich conditions, $(2\times2)\alpha$ and (6×2) structure are formed, both having As atoms at faulted sites and Ga-Ga dimers at the third atomic layer. As the As coverage is increased, the structure with Ga-As dimer $[(2\times2)\beta]$ becomes more stable, and, finally, the $c(4\times4)$ structure consisting of three As-As dimers is energetically favored at the As-rich limit. We found that the location of Mn atoms critically depends on the surface As coverage: As-deficient $(2\times2)\alpha$, (6×2) and $(2\times2)\beta$ structures have the Mn atoms at fourfold hollow sites, while the incorporation of Mn atoms into the substitutional Ga sites is enhanced in the most As-rich $c(4\times4)$ structure, in which the upper limit of substitutional Mn is 0.25 ML.

Keywords

Surface Reconstructions, Diluted Magnetic Semiconductor, Adsorption

1. Introduction

III-V compound semiconductors show a rich variety of surface reconstructions depending on the surface compositions.[1–3] The mechanism responsible for the reconstructions requires the dangling bonds of the cation and anion atoms to be empty and filled, respectively. This condition is often referred to as the electron counting model.[4] The electron counting model, together with the reduction of dangling bonds by the dimerization of surface atoms,

successfully explain a large number of atomic structures on the (001) surfaces of III-V semiconductors.[1–3]

Surface reconstructions occur also when foreign atoms are adsorbed on semiconductor surfaces at the earliest stages of heteroepitaxy. It has been widely accepted that such adsorbate-induced reconstructions are closely related to the initial processes of heteroepitaxy and the resultant interface structures.[5–13] Thus, for a more precise control of heteroepitaxy processes, a detailed understanding of their atomic geometry is prerequisite. The adsorbate-induced surface reconstructions are generally complicated, as the presence of multiple components introduces additional factors. In particular, the adsorption of Mn atoms on the GaAs(001) surface forms several types of reconstructions, depending on the preparation conditions and the amount of Mn atoms.[14–18] In this system, the surface atomic configuration is closely related with the location of Mn in GaAs.[14] Since Mn atoms at substitutional and interstitial sites in GaAs behave as hole-producing accepters and electron-producing donors, respectively, atoms in surface layers rearrange themselves so as to compensate the deficit or excess charge.

The structure identification of GaAs(001)-Mn surface is of great practical as well as fundamental interest, because the location of Mn in GaAs plays a critical role in determining the magnetic properties of Mn-doped GaAs, one of the most attractive diluted ferromagnetic semiconductors. It is now generally accepted that the ferromagnetism is mediated by holes provided by substituted Mn atoms at the Ga site,[19] while interstitial Mn atoms act as double donors, compensating free holes and hence hindering ferromagnetism.[20,21] Numerous studies have shown that the successful growth of GaMnAs films with high concentration of Mn atoms at substitutional sites can only be achieved by molecular-beam epitaxy (MBE) at low temperatures (LT).[22–25] Thus, information about the atomic processes of the Mn adsorption on GaAs under actual MBE condition is expected to provide a mechanism for controlling the location of Mn in MBE-grown GaMnAs.[22–25]

Erwin and Petukhov have studied the Mn incorporation in GaAs(001) using the den-

sity functional theory (DFT), and have found that a bulk interstitial site is energetically favorable for the Mn adsorption.[26] They also found that in the presence of the As adlayer, the energy difference between the interstitial and substitutional sites is reduced. Also, it has been predicted that Mn atoms prefer to substitute the Ga sites in GaAs under As-rich conditions.[21] However, these calculations did not take account of actual atomic structure of the surfaces. On the other hand, previous STM observations have shown that the adsorption of submonolayer of Mn on GaAs(001) induces the formation of several types of (2×2) reconstructions,[14–16] for which possible structure models have been proposed. However, to our estimation, the structure identification is not fully convincing. In addition, the surfaces studied in Refs.[14–16] were prepared by depositing Mn atoms in ultra-high vacuum (UHV) conditions, which is significantly different from actual MBE environments. We have recently studied the atomic geometry of Mn-induced surface reconstructions prepared under As-rich conditions.[17,18] We found that Mn atoms are incorporated in the substitutional Ga site under the most As-rich condition, and the interstitial site becomes more favorable as the surface As coverage is decreased. However, the mechanism for Mn incorporation is still far from being completely understood, because only As-rich phases were investigated in our earlier paper[17,18] and little is known for the atomic structures of Ga-rich phases. In addition, the critical coverage of Mn in the Mn-induced reconstructions has not yet been determined. Thus to obtain more complete understanding of the Mn incorporation in GaAs, information about the atomic structures of Mn-induced surface reconstructions in the extended range of surface stoichiometries from As-rich to Ga-rich limits is indispensable.

This paper reports a systematic study on the atomic structures of surface reconstructions on GaAs(001) induced by the adsorption of Mn. The adsorption of 0.25 monolayer (ML) of Mn atoms forms several types of reconstructions and their atomic geometry strongly depends on the surface As coverage: the structure changes from $c(4\times4)$, through $(2\times2)\beta$, to $(2\times2)\alpha$ and (6×2), as the As coverage is decreased. We show that the location of Mn atoms is closely related with the surface As coverage, providing further credence to our arguments

in the preceding paper.[17,18] In addition, we found that the upper limit of the substitutional-Mn in the As-rich $c(4\times4)$-Mn structure is 0.25 ML, at least under the present experimental conditions. On the basis of the experimental data from reflection high-energy electron diffraction (RHEED), scanning tunneling microscopy (STM) and x-ray photoelectron spectroscopy (XPS), we propose structure models with substitutional and interstitial Mn atoms, which are confirmed to be stable by first principles calculations.

2. Experimental

The experiments were performed in a MBE system which is equipped with STM and XPS apparatuses for on-line surface characterization.[3] Non-doped and nominally on-axis GaAs(001) substrates were used for the RHEED, reflectance difference spectroscopy (RDS), and XPS measurements, while Si-doped substrates were employed for the STM experiments. Cleaned GaAs(001)-(2×4) surfaces were obtained using the procedures described in our earlier paper.[3] Mn atoms were deposited on GaAs(001) at a typical rate of 0.0125 ML/s, which was calibrated by RHEED intensity oscillations measured during the growth of MnAs on GaAs(001). Here, 1 ML refers to the site-number density of the ideal GaAs(001) surface (6.26×10^{14} atoms/cm^2).

All the STM images were acquired at room temperature using electrochemically etched tungsten tips. XPS measurements were carried out using monochromatic Al Kα radiation (1486.6 eV). Photoelectrons were detected at an emission angle of 10° from the surface. The RD spectra were obtained using a modified Jobin Yvon RD spectrometer. The RDS results are commonly displayed in terms of $\Delta\tilde{r}/\tilde{r} = (\tilde{r}_{1\bar{1}0} - \tilde{r}_{110})/\tilde{r}$, where $\tilde{r}_{1\bar{1}0}$ and $\tilde{r}_{110}$ are the near-normal-incidence complex reflectances for light linearly polarized along $[1\bar{1}0]$ and [110], respectively.

RHEED rocking-curves were measured using the extended beam-rocking facility (Staib, EK-35-R and k-Space, kSA400). The energy of the incident electrons was set at 15 keV.

The glancing angle of the incident electron beam was typically changed from 0.5° to 8° with intervals of 0.03°. RHEED intensities were calculated by the multislice method proposed by Ichimiya.[27,28] Parameters used in the calculations other than the atomic coordinates were derived as described elsewhere.[3] In order to quantify the agreement between the experiments and calculations, the R factor defined in Ref.[29] was used.

3. Calculations

First-principles calculations[30,31] based on DFT[32] with the generalized gradient approximation[33] were performed. A slab geometry was used for the simple calculation, which has the supercell consisting of ten atomic layers and of vacuum region (15 Å in thickness). The cation terminated bottom layer of the slab is saturated with fictitious H atoms, which eliminate artificial dangling bonds and prevent it from coupling with the front side. The wave functions were expanded in plane waves with a kinetic energy cutoff of 16 Ry. 8×8×1 k points were used for the integration over the two-dimensional (1×1) Brillouin zones of the (2×2)β and c(4×4) surfaces and 12×12×1 k points for the (2×2)α and (6×2) surfaces. The top six layers were relaxed until all the forces were less than 0.5 eV/nm. The stability of a certain structure in the equilibrium can be determined from the surface free energy and the chemical potentials of the surface constituents, Ga and As.[34] Here, it is written as a function of the chemical potential of As with respect to its bulk As phase, μ_{As}.

STM images were calculated from the local density of states, using the Tersoff-Hamann approximation.[35,36] The tunneling current between a tip of the STM and the surface of the slab, $I(\mathbf{R})$, was obtained for the empty (filled) state using the following integration from ε_{F} to $\varepsilon_{\mathrm{F}} + eV$ ($\varepsilon_{\mathrm{F}} - eV$):

$$I(\mathbf{R}) = C \int \rho(\mathbf{R}, E) dE,$$

where ε_F is the surface Fermi energy and $\rho(\mathbf{R}, E)$ is the local density of states at the tip position, $\mathbf{R}$. Here, we set the minimum energy of the bulk conduction band as ε_{F}. At

the DFT level, band gaps are underestimated significantly, thus values of the sample bias in the STM simulation for filled-state images were corrected using the experimental band gap, 1.42 eV. The STM images were illustrated by the z-coordinate for the constant $I(\mathbf{R})$, corresponding to the condition of the constant-current mode in experiments.

4. Results and discussion

4.1. Phase Identification

We first examined the effect of the surface As coverage on the atomic structure of the Mn-induced surface reconstruction using RHEED and RDS. To control the As coverage on the GaAs(001) surface, the substrate temperature was changed from 550°C to 300°C in steps of 50°C. RHEED and RDS measurements were carried out at each step, first with the As flux (beam-equivalent pressure of 2.5×10^{-7} Torr) and then without the As flux, and the temperature was kept until the RD intensities were saturated in either case. After the measurements at a given temperature, the surfaces were exposed to the As flux again and then the temperature was decreased to the next step.

The initial (2×4) reconstruction changed to (2×2) by depositing 0.25ML of Mn at 550°C under the As flux. Figure 1(a) shows the real part of RD spectra, $\Delta r/r$ =Re$(\Delta\tilde{r}/\tilde{r})$, obtained from Mn-adsorbed GaAs(001) surfaces under the As_2 flux. While the (2×2) RHEED pattern was observed even after the As flux was interrupted at 500 and 550°C, the shape of the spectrum significantly changes, as shown in Figs.1(b)-A and 1(b)-B. Since the excess As molecules are easily desorbed from the surface at high temperatures of 500 and 550°C, the change in the RD spectrum could be ascribed to the structure change from As-rich (2×2) to Ga-rich (2×2). The Ga-rich and As-rich (2×2) reconstructions are henceforth referred to as α and β phases, respectively.

As we have already reported,[17,18] the (2×2)β phase begins to evolve into the more As-rich phase of c(4×4), as the sample was cooled under the As flux. The shape of the RD

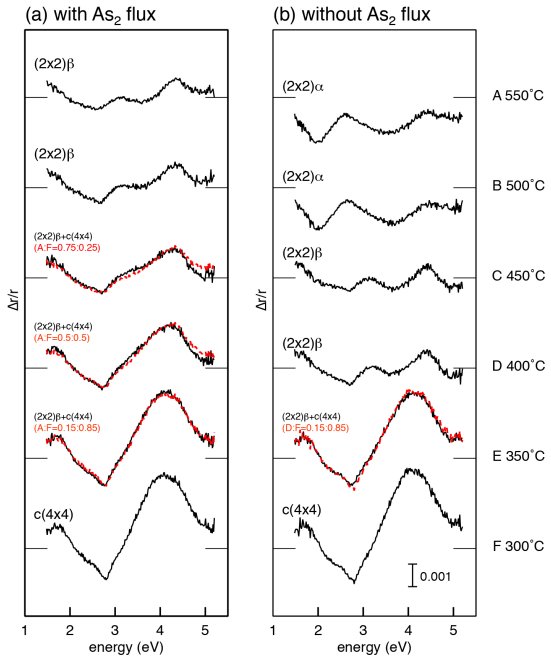

Figure 1: RD spectra measured from the Mn-adsorbed GaAs(001) surfaces (a) with and (b) without the As_2 flux of 2.5×10^{-7} Torr. Dashed curves are RD spectra synthesized from linear combinations of the $(2\times2)\beta$ [(a)-A and (b)-D] $c(4\times4)$ [(a)-F and (b)-F] spectra

.

spectrum changes as the temperature was decreased below 500°C, which corresponds to the structural change from $(2\times2)\beta$ to $c(4\times4)$. The shape of the RD spectra measured at 350, 400, and 450°C (solid curve) is well reproduced by the linear combination of the $(2\times2)\beta$ and $c(4\times4)$ surface (dashed curve). This means that no additional phase exists between $(2\times2)\beta$ and $c(4\times4)$. The $c(4\times4)$ structure, coexisting with the $(2\times2)\beta$ phase, disappeared after the As shutter was closed at 400 and 450°C, leaving the $(2\times2)\beta$ phase alone, because of the desorption of excess As. On the other hand, at lower temperatures of 300 and 350°C, the shape of the RD spectra remains almost unchanged after the As beam was turned off, indicating that the desorption of As from the $c(4\times4)$ surface is negligible below 350°C.

Figures 2(a)-2(c) show STM images and corresponding RHEED patterns taken from the $(2\times2)\alpha$ (a), $(2\times2)\beta$ (b), and $c(4\times4)$ (c) surfaces, which were prepared by closing the As shutter at 550, 450, and 300°C, respectively. Here we note that the $(2\times2)\alpha$ reconstruction is stable at temperatures above 500°C, and changes to the (6×2) reconstruction when the substrate temperature is slowly decreased below 500°C: only when the sample with the $(2\times2)\alpha$ is rapidly cooled from 500°C, could the $(2\times2)\alpha$ phase be preserved at room temperature. The filled-state STM image from the (6×2) surface is shown in Fig.2(d).

When the Mn coverage was increased above 0.25 ML, the (5×2) reconstruction was observed at 0.5 ML in the absence of the incident As flux, and the (2×2) reconstruction, which is different from $(2\times2)\alpha$ and $(2\times2)\beta$, was formed at 1.0 ML either with and without the As flux: details of these reconstructions are presently unknown. On the other hand, for the Mn coverages below 0.25 ML, the surface consists of domains of Mn-free and Mn-induced (Mn=0.25 ML) reconstructions. Since our primary interest is in the initial adsorption site of Mn, in the following, we restricted ourselves to the analysis of the surface reconstructions with 0.25 ML-Mn, and do not consider other reconstructions.

Figure 3 shows photoelectron intensity ratios of As 3d/Ga 3d for the $(2\times2)\alpha$, (6×2), $(2\times2)\beta$, and $c(4\times4)$ surfaces (squares). The data are plotted as a function of the As coverage of the structure models. The As coverages of the $(2\times2)\alpha$ and (6×2), $(2\times2)\beta$ and $c(4\times4)$-Mn

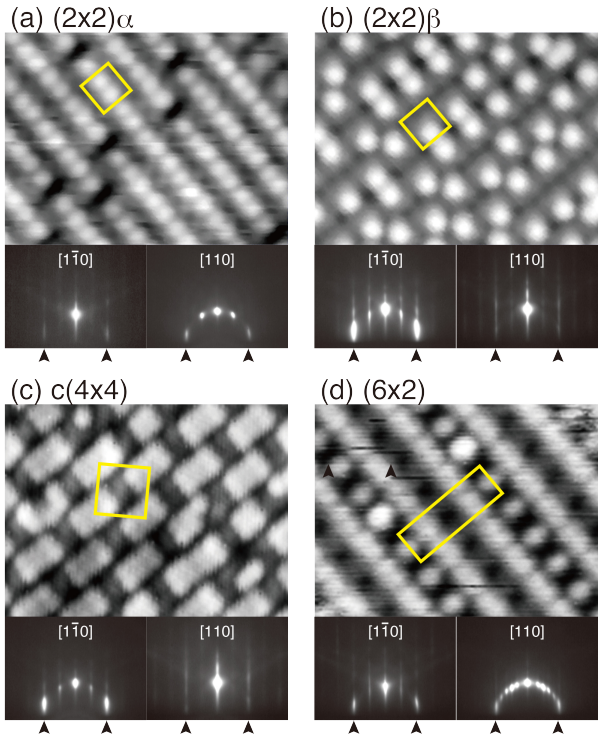

Figure 2: Typical filled-state STM images and RHEED patterns obtained from the Mn-induced surface reconstructions. (a) (2×2)α, (b) (2×2)β, (c) c(4×4), and (6×2). Image dimensions are 48 Å×64 Å. The images were taken with a sample bias of -3.0 V. The integer-order reflections in RHEED patterns are indicated by arrow heads.

models are found to be 0.5 ML, 0.5 ML, 1.0 ML, and 1.85 ML, respectively, as discussed in the following subsections; $(2\times2)\beta$ in Sec.4.2, $c(4\times4)$ in Sec.4.3, $(2\times2)\alpha$ in Sec.4.4, and (6×2) in Sec.4.5. As expected from the preparation conditions, the structure changes from $(2\times2)\alpha$ [(6×2)], through $(2\times2)\beta$, to $c(4\times4)$ with increasing As coverage.

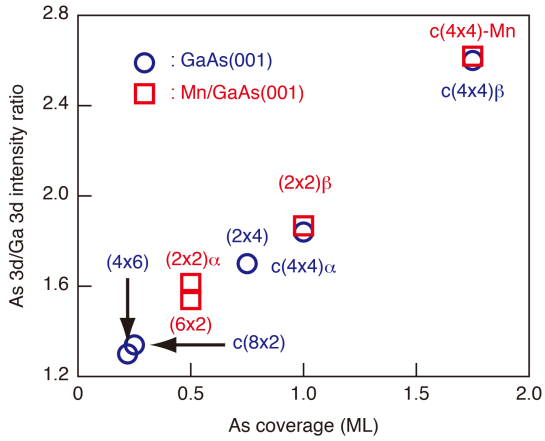

Figure 3: Photoelectron intensity ratios of As 3d/Ga 3d plotted as a function of the As coverage of the surface. Circles and squares show the results from clean and Mn-induced surface reconstructions, respectively.

4.2. As-rich $(2\times2)\beta$ reconstruction

Figures 4(a) and 4(c) show filled- and empty-state STM images, respectively, taken from the Mn-induced $(2\times2)\beta$ reconstruction. While, in the empty-state image, bright spots separated by ∼8 Å are linearly aligned along the $[1\bar{1}0]$ direction, the position is slightly (1-2 Å) shifted in the [110] and the $[\bar{1}\bar{1}0]$ directions in the filled-state image. We have already reported that the (2×2) structure with the mixed Ga-As/As-Ga dimers [Fig.4(e)] accounts for the observed STM features.[17,18]

Figures 4(b) and 4(d) show filled- and empty-state images, respectively, simulated for the structure model shown in Fig.4(e). Comparing the observed and simulated filled-state images, we found that only As atoms of Ga-As dimers are imaged in observed image [Fig.4(a)]. In the empty-state STM image, on the other hand, both As and Ga atoms appear as bright

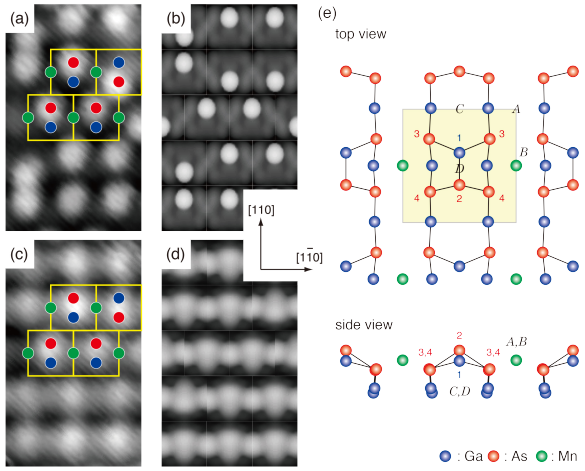

Figure 4: Typical filled-state (a) and empty-state (c) STM image obtained from the Mn-induced (2×2)β reconstruction. The images were taken with sample bias voltages of -3 V (a) and +2 V (c). (b) and (d) show simulated images for bias voltages of -3V and +2V, respectively. STM images were calculated for the (2×2) unit cell and arranged to accord with the observed images. Image dimension is 40 Å×24 Å. (e) shows the optimized model for the Mn-induced (2×2)β structure.

protrusions, which is broadly consistent with the observed features: bright spots are located at the center of dimer bonds. In addition, Mn adatoms located between the Ga-As dimers are observed as gray protrusions in both observed and simulated empty-state images.

The As coverage of the proposed model [Fig. 4(e)] is 1.0 ML, being consistent with our XPS results (Fig.3). This model consists of surface Ga-As dimers on the As-terminated surface and Mn atoms at the fourfold hollow site. The minimum energy configurations are characterized by the Mn atoms located at the B site [Fig.4(e)]. The vertical position of the Mn atom is 0.52 Å (0.61 Å) above As3 (As4) atoms. Adsorption at the A, C, and D sites are found to be higher in energy by 0.54, 0.87, and 0.42 eV per unit cell, respectively.[17,18] In good agreement with the DFT calculations, the validity of the B-site model was also supported by the RHEED rocking-curve analysis (Supporting Information, Figure S1).

The bond length of the Ga-As dimer in the optimized structure [Fig.4(e)] is 2.48 Å, which is nearly identical to that of the Mn-free GaAs(001)-$c(4\times4)\alpha$ reconstruction,[37] and close to the Ga-As bond length in bulk GaAs (2.45 Å). In this atomic geometry, the Ga-As dimer

is buckled, with the Ga atom being located at 0.71 Å below the As atom. Consequently, the Ga atom forms a planar sp^2-type bonding configuration with its As nearest neighbors: the bond angle of the surface Ga atom is 119.6° in average, which is quite close to the value expected for the ideal sp^2 arrangement.[38] On the other hand, the As atom produces p^3-type bonds with its nearest neighbors: the averaged bond angle is 98.5° and is smaller than the value 109.47° expected for an ideal sp^3 arrangement.[38] Thus, it is likely that charge transfer from Ga to As occurs in this atomic geometry. As discussed in our earlier paper,[17,18] if we assume that two electrons are donated by the adsorbed Mn atom, all of the partially-filled dangling bonds could be eliminated.

The bond lengths between atoms in the Ga-As dimers and the first layer are 2.37 Å for Ga1-As3 and 2.46 Å for As2-As4, and are rather close to the Ga-As bond length in bulk. On the other hand, the bonds between the As atoms at the first layer and Ga atoms at the second layer are slightly expanded (2.52-2.53 Å). Such a bimodal distribution in bond lengths has been found for GaAs(001)-(2×4) surface.[39]

Figure 5 shows imaginary part of the surface dielectric anisotropy of the Mn-induced surface reconstruction, $\mathrm{Im}(\Delta\varepsilon)d$, which is calculated from $\Delta\tilde{r}/\tilde{r}$ using the expression[40]

$$id\Delta\varepsilon = \frac{\Delta\tilde{r}}{\tilde{r}}\frac{\lambda}{4\pi}(\varepsilon_0 - 1),$$

where d is the effective thickness of the surface layer, ε_0 is the bulk dielectric function of GaAs,[41] and λ is the wave length of the light. The results from clean GaAs surfaces are also shown for comparison. As shown in Fig. 5(a)-C, $\mathrm{Im}(\Delta\varepsilon)d$ spectrum of $(2\times2)\beta$ is characterized by negative peaks at 2.8 eV and 4.7 eV and positive peaks at 3.1 eV, 4.4 eV, and 4.9 eV. The peak positions are close to those of the clean $c(4\times4)\alpha$ surface [Fig. 5(b)-C], which could be attributed to the existence of the Ga-As dimers in both surface structures. On the other hand, the amplitudes of the two spectra are quite different. It is reasonable to consider that the spectrum amplitudes are affected by the difference in the density of Ga-As

dimers (0.75/(1×1) for c(4×4) and 0.5/(1×1) for (2×2)β) and the existence of Mn adatoms in the (2×2)β structure.

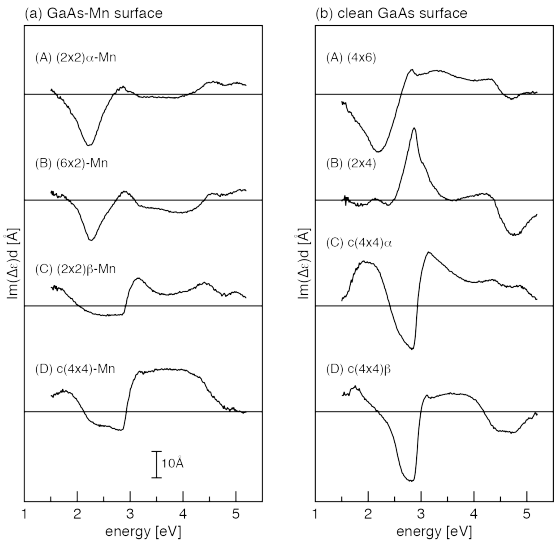

Figure 5: Imaginary part of surface dielectric anisotropy (Im($\Delta\varepsilon$)d) of the Mn-induced surface reconstructions (a) and clean surface reconstructions (b) on GaAs(001).

In the (2×2) STM image, two adjacent Ga-As dimers along the [1$\bar{1}$0] direction are often oriented in the opposite directions. Such an antiparallel configuration is slightly more stable than the parallel geometry, the difference in the formation energy being 18 meV per (2×2) unit cell. The relative density of the parallel/antiparallel geometries could be estimated by assuming the equilibrium state and the Boltzmann distribution; exp(-$\Delta E/k_{\rm B}T$), where ΔE is the difference in the formation energy per (2×2) unit cell, $k_{\rm B}$ the Boltzmann constant, and T temperature. The ratio of estimated densities is 0.45 and 0.55 for T=450°C, which is in good agreement with the STM observations (0.4:0.6).

Another interesting finding is that the (2×2) unit cells are often out of phase in adjacent rows running along the [1$\bar{1}$0] direction, resulting in the formation of a local c(2×4) unit cell. The existence of the c(2×4) structure leads to a very small energy gain [$\sim$4meV/(1×1)] compared to (2×2). Thus the formation of the phase defects is directly related to the small energy difference between the two units. On the other hand, the shift of the (2×2) cell was

not observed along the [110] direction: since the phase shift in this direction gives rise to the coexistence of the Mn atoms located at A and B sites, such an atomic arrangement is energetically unfavorable.[17,18]

4.3. As-rich $c(4\times4)$ reconstruction

As described in Sec. 4.1, the $(2\times2)\beta$ structure begins to evolve into the $c(4\times4)$ as the sample was cooled under the As_2 flux. Figure 6(a) shows a filled-state STM image of the Mn-induced $c(4\times4)$ reconstruction, in which several types of building blocks, such as (2×2), (3×2), (4×2), and $(n\times2)$ $(n>5)$, are identified. As we have already shown,[17,18] the most of unit cells have As-As dimers with the density of 94%. However, contrary to the earlier prediction,[14] the density of the (2×2) unit with one As-As dimer is less than 5%.

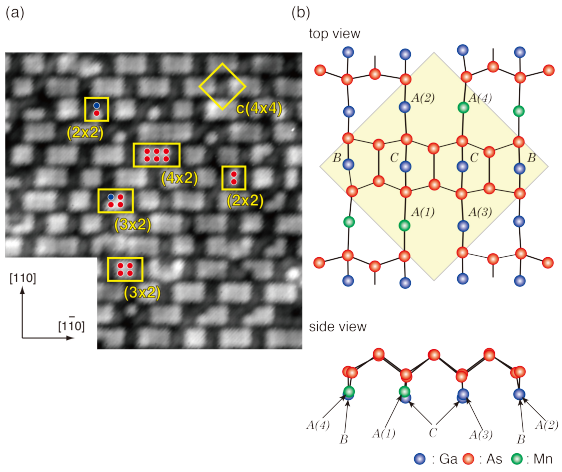

Figure 6: Typical filled-state STM image obtained from the Mn-induced $c(4\times4)$ reconstruction (a) and the structure model (b). Image dimension is 104 Å×104 Å. The image was taken with a sample bias of -3.0 V.

Shown in Fig.6(b) is the possible structure model for the $c(4\times4)$-Mn surface. For simplicity, we assumed that the $c(4\times4)$ unit consists of three As-As dimers and two Mn atoms (0.25 ML in coverage) at several substitutional sites of A, B, and C at the third atomic layer.[17,18] As expected from the similar atomic geometries of the clean $c(4\times4)\beta$ and $c(4\times4)$-

Mn reconstructions, Im($\Delta\varepsilon$)d spectra resemble each other with common spectrum features at 1.9 eV, 2.8 eV, and 3.1 eV [Figs. 5(a)-D and 5(b)-D]. Figure 7 shows relative formation energies calculated for several Mn-induced surface reconstruction models as a function of the As chemical potential. In these calculations, we set the chemical potential of Mn (μ_{Mn}) at a constant value so that no other phases (bulk Mn or MnAs) precipitate. When the Ga atoms at the A(1) and A(4) sites are substituted by the Mn atoms, the surface becomes most stable at the As-rich limit. On the other hand, the structure models with substitutional Mn atoms at B and C sites and those with Mn atoms at interstitial sites have higher energies.[17,18] These results are consistent with the RHEED analysis (Supporting Information, Figure S2).

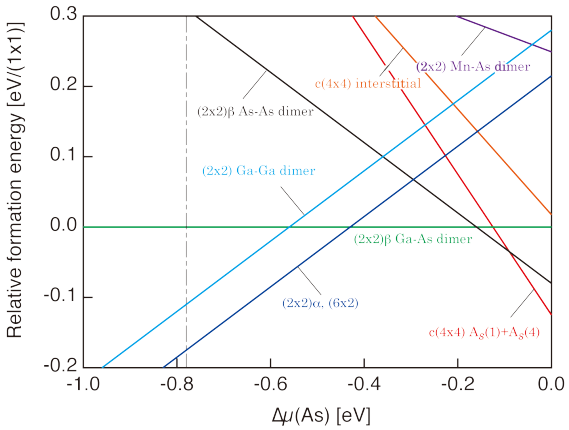

Figure 7: Relative surface energies for various Mn-induced surface reconstructions on GaAs(001) (Mn coverage = 0.25 ML) as a function of relative chemical potential of As. Thermodynamically allowed range is between -0.78 eV (Ga rich) and 0.00 eV (As rich).

In the optimized structure model (see surface structure data for coordinates), we found a small buckling of 0.14 Å in the outer dimers (bond length = 2.55 Å), while the center As-As dimer is symmetric with a bond length of 2.53 Å. These values are nearly equal to the covalent As-As bond in bulk As (2.51 Å). Each As atom in the As-As dimer is bonded to two As atoms in the second layer. The bond lengths between these atoms are calculated to be between 2.40-2.50 Å, with average bond angles of 104.1°. The length and angle of the surface As atoms calculated for the $c(4\times4)$-Mn are close to the corresponding values (105° and 2.54-2.57 Å) for the Mn-free $c(4\times4)\beta$ structure.[3]

From STM observations, the As coverage is estimated to be 1.6 ML, on the assumption that the As-As dimer is located on the ideal As-terminated GaAs(001) surface. Since, in the $c(4\times4)$-Mn structure, 0.25 ML of Ga atoms at the third layer is replaced by Mn atoms, the As coverage is increased by 0.25 ML. The resultant value of 1.85 ML is in good agreement with our XPS measurements: as shown in Fig.3, the surface As coverage of the $c(4\times4)$-Mn surface is close to the value for the GaAs(001)-$c(4\times4)\beta$ structure (1.75 ML).

In the proposed $c(4\times4)$-Mn model, substitutional Mn has two possible valence states: divalent (Mn^{2+}) and trivalent (Mn^{3+}) states, which have 1 and 0 holes, respectively. Thus, if the valence state of Mn is Mn^{2+}, the $c(4\times4)$-Mn model does not satisfy the electron counting requirements.[4] However, our first-principles calculations show that one of the five $3d$ electrons, together with two $4s$ electrons, are consumed to the formation of covalent bonds between the substituted Mn and its nearest neighbor As atom, so that the $c(4\times4)$-Mn model agrees with electron counting heuristics.[15,42] This is in good agreement with the calculated spin magnetic moment of $4\mu_B$/Mn. On the other hand, as mentioned earlier, the Mn atom located at the interstitial site in the $(2\times2)\beta$ structure donates two $4s$ electrons to stabilize the surface, while leaving five $3d$ electrons intact. The calculated spin magnetic moment is $5\mu_B$/Mn. These results are consistent with the band structure calculations: both $(2\times2)\beta$ and $c(4\times4)$-Mn structures are indeed semiconducting with an energy gap.

The present results show that the substitutional incorporation of Mn (0.25ML) in GaAs is facilitated as the surface As coverage is increased. On the other hand, higher concentrations of substitutional Mn atoms in GaMnAs films can only be achieved by MBE at LT.[22–25] The LT-MBE growth usually proceeds under the As-rich conditions and the growing GaMnAs surface shows a (1×2)-like RHEED patterns,[22–25] similar to those shown in Fig. 2(c). Thus, while no definitive conclusion is available without detailed analysis on the growing GaMnAs surface, it is plausible to consider that the substitutional incorporation of Mn in GaMnAs growth occurs with the formation of the $c(4\times4)$-like reconstruction at the growth front.

Here, one may raise the question as to whether it is possible to increase the Mn concen-

tration above 0.25 ML. Thus, we have investigated the critical amount of substitutional-Mn atoms using the samples with Mn coverages ranging from 0.25 to 1.0 ML. The samples were prepared by cooling to 300°C under the As_2 flux after the deposition of Mn at 550°C. As shown in Figs. 8(b)-8(d), for Mn coverages above 0.375 ML, MnAs islands are formed on the $c(4\times4)$ surface, which was also confirmed by RHEED observations. On the other hand, such islands are hardly observed on the surface below 0.25 ML [Fig. 8(a)]. This means that the upper limit of the substitutional-Mn in the $c(4\times4)$-Mn structure is 0.25 ML, at least under the present experimental condition, beyond which the excess Mn atoms are consumed in the formation of MnAs islands. This value is significantly smaller than that ($\sim$1 ML) in the Mn δ-doped GaAs sample.[43,44] We point out that Mn atoms are localized in the single atomic layer in the $c(4\times4)$-Mn structure, while Mn atoms are distributed over 2-5 ML in the δ-doped sample.[43–45]

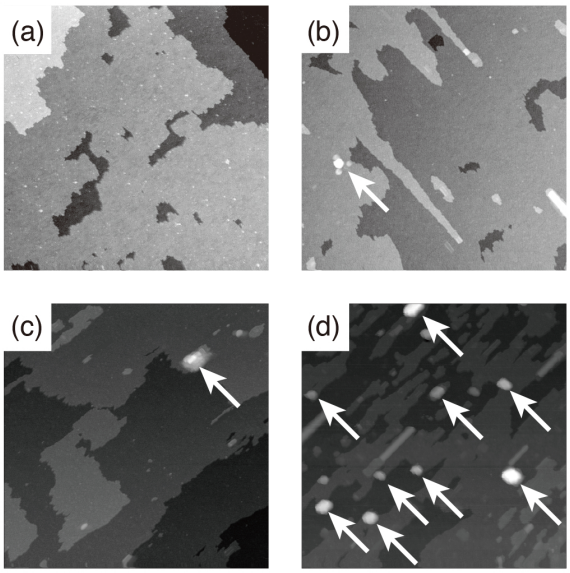

Figure 8: Typical filled-state STM images obtained from the Mn-induced $c(4\times4)$ reconstructions with Mn coverages of 0.25 ML (a), 0.375 ML (b), 0.5 ML (c), and 1.0 ML (d). Arrows indicate MnAs islands. Image dimension is 2000 Å×2000 Å. The image was taken with a sample bias of -3.0 V.

4.4. Ga-rich (2×2)α reconstruction

Previous DFT calculations have predicted that the (2×2) structure with the Ga-Ga dimer becomes stable under more Ga-rich conditions.[14] Since the STM image of the (2×2)α surface shows pairs of bright spots aligned in the [110] direction, as shown in Fig.2(a), one may speculate that the bright spots correspond to Ga atoms of surface Ga dimers. However, the separation of the two bright spots is ∼3.5 Å, which is incompatible with the formation of dimers. To obtain the details of the Ga-rich (2×2)α structure, it is necessary to assign the atomic site to which each bright spot is attributed. Although it is not *a priori* clear to which protrusions a STM image correspond, in this case, the lattice sites of the (2×2)α surface can be assigned, connecting the Ga-As dimer structure of the (2×2)β phase. For this purpose, we prepared the (2×2)α surface coexisting with the (2×2)β structures. Figure 9(a) shows a filled-state STM image taken from the sample prepared by closing the As shutter at 490°C. By superimposing the (1×1) lattice mesh over the image (Fig.9), it turns out that the bright spots [crosses in Fig.9(b)] in the (2×2)α phase are located at the positions shifted by ∼2 Å along the [110] direction from the surface As atoms (small circles) in the (2×2)α area. Thus, it is suggested that the (2×2)α surface contains surface atoms at faulted sites relative to their bulk positions, which manifest themselves as bright spots in Fig.9(a). Such structural features are clearly incompatible with the Ga-Ga dimer model.

The existence of surface As atoms at faulted sites was found in the Ga-rich reconstructions of (6×6),[46,47] c(8×2),[48,49] and (4×6),[50] in which Ga atoms at the subsurface layers form dimers. Since, as shown in Figs. 5(a)-A and 5(b)-A, Im($\Delta\varepsilon$)d spectrum of (2×2)α is similar to that of the clean (4×6) surface, it is plausible to consider that the (2×2)α structure also consists of the faulted As atoms and subsurface dimer. Thus, we propose a structure model for (2×2)α, as shown in Fig.10(a). This model is characterized by faulted As atoms, Mn atoms at interstitial sites, and Ga-Ga dimers at the third atomic layer. As shown in Fig.7, the proposed model (blue line) has an energy lower by 0.065 eV/(1×1) relative to the Ga-Ga dimer model proposed in Ref.[14] (light-blue line). The As coverage of the proposed model is

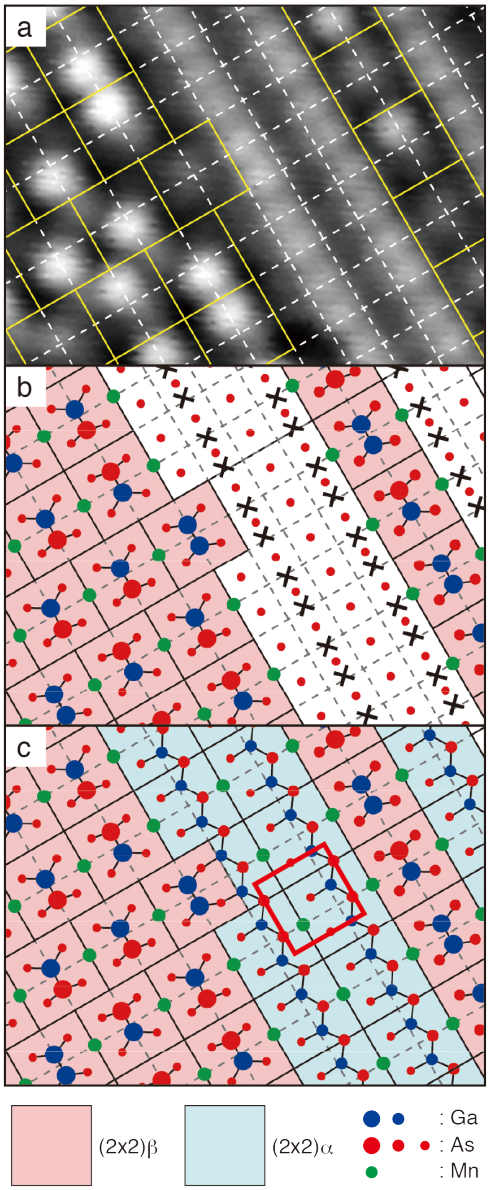

Figure 9: (a)Filled-state STM image obtained from the coexisting phases of (2×2)α and (2×2)β. Image dimensions are 36 Å×48 Å. The images were taken with a sample bias of -3.0 V. Atomic positions are indicated in (b) and (c). Solid and dashed lines indicate the (2×2) and (1×1) lattice meshes, respectively. The square in (c) corresponds to the (2×2) unit cell in Fig. 10(a).

0.5 ML, in good agreement with the XPS result (Fig.3).

The atomic positions of the (2×2)α and (2×2)β structures are indicated in Fig.9(c). It is clearly seen that the Mn atoms are arranged with a (2×2) periodicity, which is often continued over the boundary between the (2×2)α and (2×2)β phases. This means that the rearrangement of Mn atoms is not required for the structure change between the (2×2)α and (2×2)β phases. Another noteworthy finding is the occasional existence of the (2×2)β unit with the Ga-Ga dimer which manifests itself as a darker spot located at the center of the unit cell. The density of the Ga-Ga dimer unit is much lower than that of (2×2)α structure, which is broadly consistent with its higher formation energy (Fig.7).

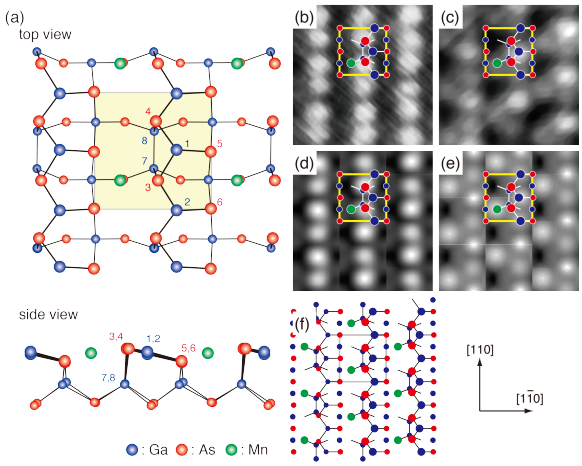

Figure 10: (a) Optimized structure model for (2×2)α. Typical filled-state (b) and empty-state (c) STM image obtained from the Mn-induced (2×2)α reconstruction. The images were taken with sample bias voltages of -3 V (b) and +2 V (c). (d) and (e) show simulated images for bias voltages of -3 V and +2 V, respectively. Image dimension is 24 Å×24 Å. The structure model in (f) are obtained by arranging the (2×2)α unit cell to accord with the observed images [(b) and (c)].

The largest displacements in the proposed model [Fig.10(a)] are observed for the faulted As atoms along the [110] direction, resulting in the formation of third-layer Ga-Ga dimers with a bond length of 2.56 Å. Here, we note that the chemical bonds are formed between the Ga atoms constituting third-layer Ga dimers and surface As atoms at faulted sites: the bond lengths are 2.50 Å (As3-Ga7) and 2.59 Å (As4-Ga8), which are smaller than the

corresponding values for the $c(8\times2)$ surface (experimental value: 2.72 Å, theoretical value: 2.66 Å),[51] and rather close to the Ga-As distance in bulk GaAs. Since the Ga7 and Ga8 atoms are bound with three As atoms and one Ga atom, the Ga-Ga dimer would result in a deficit of a $\frac{1}{2}$ electron per dimer. The threefold-coordinated surface Ga atoms are displaced downward by large amounts of 0.69 Å (Ga1) and 0.86 Å (Ga2), to achieve an almost perfect planar sp^2 configuration with averaged bond angles of 119° (Ga1) and 120° (Ga2). The surface Ga atom has an excess $\frac{3}{4}$ electron, while the three-coordinated surface As atoms at faulted (As3 and As4) and unfaulted sites (As5 and As6) have a dangling bond with a $\frac{5}{4}$ electron. Since the Mn atom donates two electrons, charge transfer from two surface-Ga atoms ($2\times\frac{3}{4}=\frac{3}{2}$ electrons) and the Mn atom (2 electrons) to the third-layer Ga dimer and four surface-As atoms transforms the As- and Ga- dangling bonds into fully occupied and empty states, respectively, leaving any partially filled dangling bonds.[4] Similarly to the case for $(2\times2)\beta$, the $(2\times2)\alpha$ structure is semiconducting, and five $3d$ electrons remain intact (the calculated spin magnetic moment of this model is $5\mu_B$/Mn).

Figures 10(b) and 10(c) show STM images taken with sample bias voltages of -3 V and +2 V, respectively. A unit cell is positioned at identical locations on both images. Shown in Figs. 10(d) and 10(e) are simulated STM images for the optimized structure [Fig.10(a)]. From the comparison of the observed and simulated images, it turns out that As atoms at faulted sites correspond to the bright spots in the filled-state image and that the As atoms at the unfaulted sites are observed as much less bright features. Such a difference could be explained by considering the vertical positions of the two-types of As atoms: the faulted As atoms are located at 0.93 Å higher than their ideal bulk positions, while unfaulted As atoms are vertically displaced by a small amount of 0.01-0.09 Å. As a result of larger atomic displacements, the faulted As atoms have a bond angle of 92°, which is significantly smaller than those for unfaulted atoms (100-102°). In the empty-state image, on the other hand, the bright protrusions come from empty state of the Ga1 atom and the gray protrusions correspond to the Ga2 and Mn atoms. Since the Ga1 atom is located above the subsurface

Ga-Ga dimer, the combination of STM observations and simulations enables us to obtain the information about the atomic positions of subsurface Ga-Ga dimers.

Figure 11 shows RHEED rocking curve measured from the (2×2)α surface at 550°C, together with the calculated ones using the atomic coordinates obtained by DFT calculations (see surface structure data for coordinates). In the present RHEED analysis, the $\frac{1}{2}$-order reflections for the [1$\bar{1}$0]-incidence were excluded, because of their elongated feature [Fig.2(a)].[52,53] Parameters used for the RHEED calculations are the same as those for the (2×2)β. The shape of the measured rocking curves is well reproduced by the calculations for the model shown in Fig.10(f) with an R-factor of 0.153.

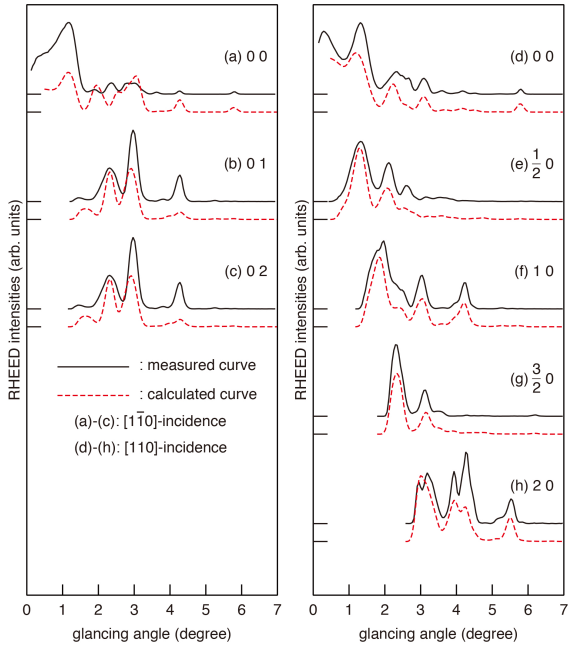

Figure 11: RHEED rocking curve (solid curves) measured from the Mn-induced (2×2)α surface at 550°C. The dashed curves are calculated using the atomic coordinates obtained by first-principles calculations for the structure model shown in Fig.10(f).

4.5. Ga-rich (6×2) reconstruction

As mentioned in Sec. 4.1, the (2×2)α structure is stable only at temperatures higher than 500°C, and begins to evolve into the (6×2) one below 500°C. To obtain the well-ordered

(6×2) surface, the sample was prepared by interrupting the As molecular beam at 550°C and then kept at 430°C for 1000s. The surface showed a distinct (6×2) RHEED pattern. Figure 12(a) shows a filled-state STM image taken from the (6×2) reconstruction. Pairs of bright spots running along the [110] direction are aligned in two 12-Å distanced lines in Fig.12(a); the two lines are separated by the dots of the broken rows. The spacing of the dots along the [110] directions is 8 Å in average, corresponding to the 2× periodicity.

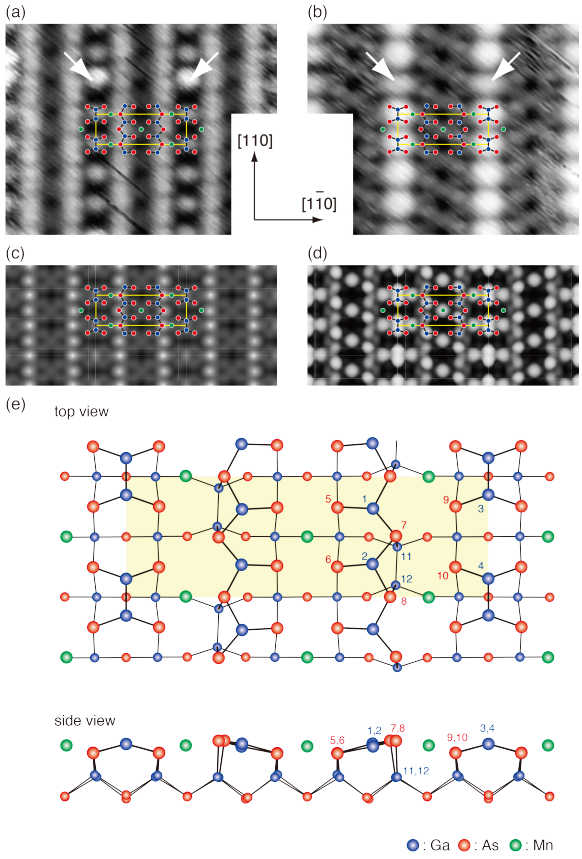

Figure 12: Typical filled-state (-3V) (a) and empty-state (+2V) (b) STM images obtained from the Mn-induced (6×2) reconstruction. Image dimension is 56 Å×72 Å. Arrows indicate the positions where Ga-Ga dimers at the first layer are replaced by Ga-As dimers. Simulated filled-state (c) and empty-state (d) images. (e) shows the optimized structure model.

As shown in Fig.5(a) the shape of the Im($\Delta\varepsilon$)d spectrum for the (6×2) surface (B) closely resembles that for (2×2)α (A) and the As/Ga XPS ratios for (6×2) nearly equals the value of (2×2)α (Fig. 3). Thus, it is likely that the (6×2) and (2×2)α structures consist of common

structure elements. While several possible models containing these structure elements were considered, only the model shown in Fig. 12(e) could account for the observed STM features. The surface As coverage of this model is exactly the same as that of (2×2)α (0.5 ML). In addition to structure elements common with the (2×2)α (subsurface dimerization, As atoms at faulted sites, and Mn atoms at hollow sites), the proposed (6×2) model has the Ga-Ga dimers at the first atomic layer. This model satisfies the electron counting requirement,[4] and has the same formation energy as the (2×2)α model within 0.005 eV per (1×1) unit cell, as shown in Fig.7. The energetic degeneracy of the two phases is consistent with the experimental finding that the structure change between (6×2) and (2×2)α is reversible: when the (6×2) surface was heated to above 500°C without the As_2 flux, the (6×2) surface rearranged to (2×2)α. The proposed (6×2) model turns out to be semiconducting and is in agreement with the electron counting rule.[4,15,42] The calculated spin magnetic moment is $5\mu_B$/Mn, indicating that five $3d$ electrons do not participate in the bonding.

Shown in Figs. 12(c) and 12(d) are simulated filled- and empty-state STM images for the proposed structure model [Fig. 12(e)]. Comparing the observed filled-state image [Fig. 12(a)] with the simulated one [Fig. 12(c)], we found that the faulted As atoms (As7 and As8), located at 0.79-0.86 Å higher than unfaulted As atoms (As5, As6, As9, and As10), correspond to the bright lines running along the [110] directions in the filled-state STM image [Fig.12(a)], similarly to the case for (2×2)α. The dot-like features, which correspond to the Ga-Ga dimer at the first atomic layer, are observed in both filled- and empty-state images. This is in marked contrast with the naive interpretation of STM images for GaAs surfaces: the dangling bonds of surface As and Ga atoms are imaged in the filled- and empty-state images, respectively. Similar STM observations have been reported for GaAs(001)-(2×4) surface, in which surface As-As dimers are imaged irrespective of the bias polarity.[54] According to the interpretation in ref.[54] , the present results could be explained by assuming that tunneling occurs predominantly from bonding orbitals of Ga-Ga dimer and that filled-states of As atoms located lower than surface Ga atoms are hardly accessed at negative sample bias.

However, further studies are needed to support this conjecture.

The proposed (6×2) unit cell is asymmetric with respect to the [110] direction. Such an asymmetric feature is clearly seen in the observed [Fig. 12(b)] and simulated [Fig. 12(d)] empty-state images: similar to the case for the (2×2)α model, the Ga2 atom located above the subsurface Ga-Ga dimer manifests itself as a brighter protrusion than Ga1 atom. As seen in these figures, there exist two types of asymmetric unit cells, which gives rise to symmetric (6×2) RHEED patterns observed along the [110] direction.

The distance between Ga atoms constituting third-layer Ga-Ga dimer (Ga11 and Ga12) and As atoms at faulted sites (As7 and As8) falls in the range of 2.50-2.58 Å, and is compatible with the existence of a chemical bond between these atoms. This bond formation is indispensable to satisfy the electron counting requirement, as in the case for (2×2)α.[4] The bond length of Ga-Ga dimers amounts to 2.44 Å in the first-atomic layer and to 2.55 Å in the third layer.

As indicated by white arrows in Figs.12(a) and 12(b), the 2× periodicity in the dot-like features is often disturbed. Such a local disorder is caused by the coexistence of Ga-As dimers with Ga-Ga dimers. Each Ga-Ga dimer shows a single protrusion in both filled- and empty-state STM images. On the other hand, since As (Ga) atoms manifest themselves as brighter spots in filled- (empty-) state STM images, the Ga (As) atom of Ga-As dimer is imaged in empty- (filled-) state image, so that the positions of bright spots are slightly shifted (∼1 Å) along the [110] or [$\overline{1}\overline{1}$0] direction, as can be seen in Figs.12(a) and 12(b). We note that the structure model having the Ga-As dimer, instead of the Ga-Ga dimer, also agrees with the electron counting heuristics.[4]

Figure 13 shows the measured (solid curves) and calculated (dashed curves) RHEED rocking curves. Fifty fractional-order and 11 integer-order reflections were used for the calculation along the [110] direction, and ten fractional-order and 11 integer-order reflections were used for the [1$\overline{1}$0] incidence azimuth: As in the case for (2×2)α, the streaky $\frac{1}{2}$-order reflections along the [1$\overline{1}$0] direction [Fig.2(d)] were excluded from the present RHEED analysis.

The atomic coordinates obtained by DFT calculations were used in the RHEED calculations (see Ref. surface structure data for coordinates). The R factor for the proposed model is 0.131, showing a good agreement between the experiments and calculations.

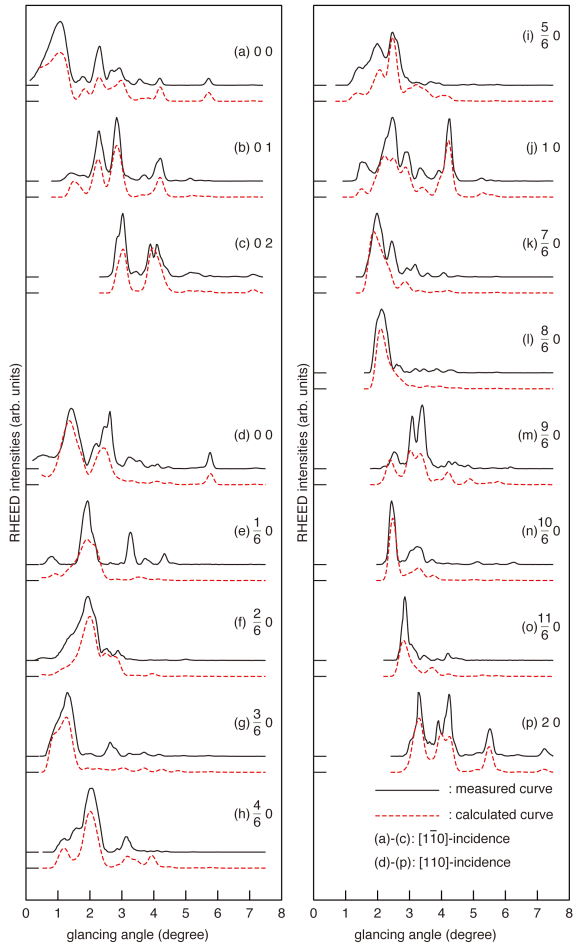

Figure 13: RHEED rocking curve (solid curves) measured from the Mn-induced (6×2) surface. The dashed curves are calculated using the atomic coordinates obtained by first-principles calculations for the structure model shown in Fig.12(c).

As mentioned earlier, (6×2) surface was obtained by slowly cooling the (2×2)α surface below 500°C, while the structure change was kinetically suppressed by quenching the (2×2)α sample. The difference in the structure models between (6×2) and (2×2)α is the existence of the top-layer Ga-Ga dimers on the (6×2) surface, which manifest themselves as dot-like features in the STM images. Here, it is interesting to note that the spectrum shape of the

surface dielectric anisotropies (Im($\Delta\varepsilon$)d) shown in Fig.5(a)-A and 5(a)-B is insensitive to the difference in the Ga-Ga dimer density. Figure 14 compares STM images obtained after the (2×2)α surfaces were cooled with different rates. The surfaces shown in Figs.14(a) and 14(c) correspond to (2×2)α and (6×2) phases, respectively, and the surface (b) corresponds to the intermediate state in between. As we have expected, the density of Ga-Ga dimer depends on the cooling rate of the (2×2)α surface: the coverages of Ga atoms constituting the Ga-Ga dimer are estimated to be 0.06 ML, 0.10 ML, and 0.20 ML in Figs.14(a), 14(b), and 14(c), respectively. The values of the (2×2)α and (6×2) surface are slightly different from those estimated from the ideal models (0 ML and 0.167 ML). The discrepancy for (2×2)α could be explained by considering that the formation of the Ga-Ga dimer in the (2×2)α matrix could not be fully suppressed even when the sample was quenched. For (6×2), on the other hand, carefully observing the image in Fig.14(c) we found the local c(8×2) unit also exists on the (6×2) surface. Since the density of the Ga-Ga dimer in the c(8×2) unit (0.25 ML) is higher than that in (6×2) (0.167 ML), the coexistence of the c(8×2) units with (6×2) results in the increase of the Ga-Ga dimer density.

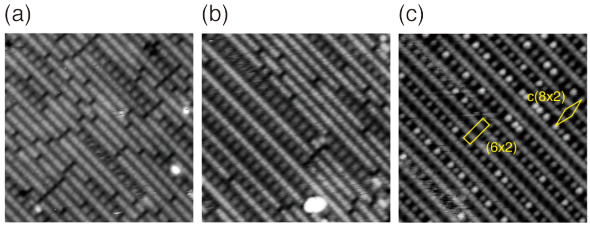

Figure 14: Filled-state STM images obtained after the (2×2)α surface was cooled from 550°C to room temperature without the As_2 flux. The images (a) and (b) were obtained when the substrate temperature was rapidly (∼1°C/s) and slowly (∼0.3°C/s) cooled, respectively. The sample (c) was prepared by slowly cooling from 550°C and then kept at 430°C for 1000s. The images were taken with a sample bias of -3.0 V. Image dimension is 165 Å×165 Å.

5. Conclusions

We have studied the atomic structures and their stability of the Mn-induced surface reconstructions on GaAs(001). The experimental data show the sequence of surface structures as a function of As coverage, in good agreement with the DFT calculations: $(2\times2)\alpha/(6\times6)$, $(2\times2)\beta$, and $c(4\times4)$. We have demonstrated that Mn atoms change their adsorption site depending on the surface As coverage: Mn atoms substitute the subsurface Ga-sites in the most As-rich $c(4\times4)$ reconstruction, and are incorporated into interstitial sites in the moderate As-rich $(2\times2)\beta$, and Ga-rich (6×6) and $(2\times2)\beta$ structures.

Despite considerable efforts, the highest Curie temperature (T_c) for GaMnAs is below room temperature (< 200K), and practical applications of this material will require much higher value. For further improvements, it is essential to control the incorporation of Mn in GaMnAs growth at an atomic level, because the increase of T_c is closely related with the location of Mn in GaAs.[19] The fundamental understanding of the Mn-induced surface reconstructions on GaAs, acquired in this study, is one of the most primitive and important factors to control the atomic process of GaMnAs growth. Thus, the present results will offer a strategy to achieve the high concentration of substitutional Mn atoms in GaMnAs for practical applications in spintronic devices.

Acknowledgement

We are indebted to T. Hanada for use of the RHEED intensity calculation program. Helpful discussions with M. Hirayama and Y. Kanno are gratefully acknowledged. This work was partially supported by the Ministry of Education, Science, Sports, and Culture, Grant-in-Aid for Scientific Research (B) (Grant No. 22360020)

Supporting Information Available

RHEED rocking curves for the Mn-induced (2×2)β and c(4×4) reconstructions (PDF) Atomic coordinates of surface structures (CIF).

This material is available free of charge via the Internet at `http://pubs.acs.org/`.

References

(1) Xue, Q.-K.; Hashizume, T.; Sakurai, T. Scaninng Tunneling Microcopy of III-V Compound Semiconductor (001) Surfaces. *Prog. Surf. Sci.* **1997**, *56*, 1-132 .

(2) LaBella, V.P.; Krause, M.R.; Ding, Z.; Thbado, P.M. Arsenic-Rich GaAs(001) Surface Structure. *Surf. Sci. Rep.* **2005**, *60*, 1-53 .

(3) Ohtake, A. Surface Reconstructions on GaAs(001). *Surf. Sci. Rep.* **2008**, *63*, 295-327 .

(4) Pashley, M.D. Electron Counting Model and its Application to Island Structures on Molecular-Beam Epitaxy Grown GaAs(001) and ZnSe(001). *Phys. Rev. B* **1989**, *40*, 10481-10487 .

(5) Ohtake, A.; Miwa, S.; Kuo, L.H.; Yasuda, T.; Kimura, K.; Jin, C.G.; Yao, T. Characterization and Control of II-VI/III-V Heterovalent Interfaces. *J. Cryst. Growth* **1998**, *184/185*, 163-172 .

(6) Xie, Q.; Van Nostrand, J.E.; Brown, J.L.; Stutz, C.E. Arsenic for Antimony Exchange on GaSb, its Impacts on Surface Morphology, and Interface Structure. *J. Appl. Phys.* **1999**, *86*, 329-337 .

(7) Ohtake, A.; Mano, T.; Hagiwara, A.; Nakamura, J. Self-Assembled Growth of Ga Droplets on GaAs (001): Role of Surface Reconstructions. *Cryst. Growth Des.* **2014**, *14*, 3110-3115 .

(8) Yasuda, T.; Miyata, N.; Ohtake, A. Influence of Initial Surface Reconstruction on the Interface Structure of HfO_2/GaAs(001), *Appl. Surf. Sci.* **2008**, *254*, 7565-7568 .

(9) Omi, H.; Saito, H.; Osaka, T. Polarity Propagation in the InSb/α-Sn/InSb Heterostructure. *Phys. Rev. Lett.* **1994**, *72*, 2596-2599 .

(10) Heun, S.; Sugiyama, M.; Maeyama, S.; Watanabe, Y.; Wada, K.; Oshima, M. Growth of Si on Different GaAs Surfaces: A Comparative Study. *Phys. Rev. B* **1996**, *53*, 13534-13541 .

(11) Ohtake, A.; Mitsuishi, K. Polarity Controlled InAs{111} Films Grown on Si(111), *J. Vac. Sci. Technol. B* **2011**, *29*, 031804 .

(12) Wang, R.; Boschker, J.E.; Bruyer, E.; Di Sante, D.; Picozzi, S.; Perumal, K.; Giussani, A.; Riechert, H.; Calarco, R. Toward Truly Single Crystalline GeTe Films: The Relevance of the Substrate Surface. *J. Phys. Chem. C* **2014**, *118*, 29724-29730 .

(13) Boschker, J.E.; Momand, J.; Bragaglia, V.; Wang, R.; Perumal, K.; Giussani, A.; Kooi, B.J.; Riechert, H.; Calarco, R. Surface Reconstruction-Induced Coincidence Lattice Formation Between Two-Dimensionally Bonded Materials and a Three-Dimensionally Bonded Substrate. *Nano Lett.* **2014**, *14*, 3534-3538 .

(14) Zhang, S.B.; Zhang, L.; Xu, L.; Wang, E.G.; Liu, X.; Jia, J.-F.; Xue, Q.-K. Spin Driving Reconstructions on the GaAs(001):Mn Surface. *Phys. Rev. B* **2004**, *69*, 121308(R) .

(15) Zhang, L.; Wang, E.G.; Xue, Q.K.; Zhang, S.B.; Zhang, Z. Generalized Electron Counting in Determination of Metal-Induced Reconstruction of Compound Semiconductor Surfaces. *Phys. Rev. Lett.* **2006**, *97*, 126103 .

(16) Colonna, S.; Placidi, E.; Ronci, F.; Cricenti, A.; Arciprete, F.; Balzarotti, A. The Role of Kinetics on the Mn-Induced Reconstructions of the GaAs(001) Surface. *J. Appl. Phys.* **2011**, *109*, 123522 .

(17) Ohtake, A.; Hagiwara, A.; Nakamura, J. Controlled Incorporation of Mn in GaAs: Role of Surface Reconstructions. *Phys. Rev. B* **2013**, *87*, 165301 .

(18) Ohtake, A.; Hagiwara, A.; Nakamura, J. Erratum: Controlled Incorporation of Mn in GaAs: Role of Surface Reconstructions. *Phys. Rev. B* **2013**, *87*, 159910(E) .

(19) Dietl, T.; Matsukura, F.; Cibert, J.; Ferrand, D. Zener Model Description of Ferromagnetism in Zinc-Blende Magnetic Semiconductors. *Science* **2000**, *287*, 1019-1022 .

(20) Máca F.; Mašek, J. Electronic states in $Ga_{1-x}Mn_xAs$: Substitutional Versus Interstitial Position of Mn. *Phys. Rev. B* **2002**, *65*, 235209 .

(21) Mahadevan, P.; Zunger, A. Ferromagnetism in Mn-Doped GaAs due to Substitutional-Interstitial Complexes. *Phys. Rev. B* **2003**, *68*, 075202 .

(22) Ohno, H.; Shen, A.; Matsukura, F.; Oiwa, A.; Endo, A.; Katsumoto, S.; Iye, Y. A New Diluted Magnetic Semiconductor based on GaAs. *Appl. Phys. Lett.* **1996**, *69*, 363-365 .

(23) Ohya, S.; Ohno, K.; Tanaka, M. Magneto-Optical and Magnetotransport Properties of Heavily Mn-Doped GaMnAs. *Appl. Phys. Lett.* **2007**, *90*, 112503 .

(24) Mack, S.; Myers, R.C.; Heron, J.T.; Gossard, A.C.; Awschalom, D.D. Stoichiometric Growth of High Curie Temperature Heavily Alloyed GaMnAs. *Appl. Phys. Lett.* **2008**, *92*, 192502 .

(25) Chiba, D.; Nishitani, Y.; Matsukura, F.; Ohno, H. Properties of $Ga_{1-x}Mn_xAs$ with High Mn Composition (x>0.1). *Appl. Phys. Lett.* **2007**, *90*, 122503 .

(26) Erwin, S.C.; Petukhov, A.G. Self-Compensation in Manganese-Doped Ferromagnetic Semiconductors. *Phys. Rev. Lett.* **2002**, *89*, 227201 .

(27) Ichimiya, A. Many-Beam Calculation of Reflection High-Energy Electron Diffraction (RHEED) Intensities by the Multi-Slice Method. *Jpn. J. Appl. Phys., Part 1* **1983**, *22*, 176-180; *Jpn. J. Appl. Phys., Part 1* .

(28) Ichimiya, A. Correction to "Many-Beam Calculation of Reflection High-Energy Electron Diffraction (RHEED) Intensities by the Multi-Slice Method". *Jpn. J. Appl. Phys., Part 1* **1985**, *24*, 1365 .

(29) Hanada, T.; Daimon, H.; Ino, S. Rocking-Curve Analysis of Reflection High-Energy Electron Diffraction from the Si(111)-($\sqrt{3} \times \sqrt{3}$)$R30°$-Al, -Ga, and -In Surfaces. *Phys. Rev. B* **1995**, *51*, 13320-13325 .

(30) Vanderbilt, D. Soft Self-Consistent Pseudopotentials in a Generalized Eigenvalue Formalism. *Phys. Rev. B* **1990**, *41*, 7892-7895 .

(31) Yamauchi, J.; Tsukada, M.; Watanabe, S.; Sugino, O. First-Principles Study on Energetics of c-BN(001) Reconstructed Surfaces. *Phys. Rev. B* **1996**, *54*, 5586-5603 .

(32) Hohenberg, P.; Kohn, W. Inhomogeneous Electron Gas. *Phys. Rev.* **1964**, *136*, B864-B871 .

(33) Perdew, J.P.; Burke, K.; Ernzerhof, M. Generalized Gradient Approximation Made Simple. *Phys. Rev. Lett.* **1996**, *77*, 3865-3868 .

(34) Moll, N.; Kley, A.; Pehlke, E.; Scheffler, M. GaAs Equilibrium Crystal Shape from First Principles. *Phys. Rev. B* **1996**, *54*, 8844-8854 .

(35) Bardeen, J. Tunnelling from a Many-Particle Point of View. *Phys. Rev. Lett.* **1961**, *6*, 57-59 .

(36) Tersoff, J.; Hamann, D.-R. Theory of the Scanning Tunneling Microscope. *Phys. Rev. B* **1985**, *31*, 805-813 .

(37) Ohtake, A.; Nakamura, J.; Tsukamoto, S.; Koguchi, N.; Natori, A. New Structure Model for the GaAs(001)-$c(4\times4)$ Surface. *Phys. Rev. Lett.* **2002**, *89*, 206102 .

(38) Ohtake, A.; Nakamura, J.; Komura, T.; Hanada, T.; Yao, T.; Kuramochi, H.; Ozeki, M. Surface Structures of GaAs{111}A,B-(2×2). *Phys. Rev. B* **2001**, *64*, 045318 .

(39) Schmidt, W.G.; Bechstedt, F. Geometry and Electronic Structure of GaAs(001)(2×4) Reconstructions. *Phys. Rev. B* **1996**, *54*, 16742-16748 .

(40) Aspnes, D.E. Above-Bandgap Optical Anisotropies in Cubic Semiconductors: A Visible-Near Ultraviolet Probe of Surfaces. *J. Vac. Sci. Technol. B* **1985**, *3*, 1498-1506 .

(41) Aspnes, D.E.; Studna, A.A. Dielectric Functions and Optical Parameters of Si, Ge, GaP, GaAs, GaSb, InP, InAs, and InSb from 1.5 to 6.0 eV. *Phys. Rev. B* **1983**, *27*, 985-1009 .

(42) Yang, S.; Zhang, L.; Chen, H.; Wang, E.; Zhang, Z. Generic Guiding Principle for the Prediction of Metal-Induced Reconstructions of Compound Semiconductor Surfaces. *Phys. Rev. B* **2008**, *78*, 075305 .

(43) Nazmul, A.M.; Sugahara, S.; Tanaka, M. MBE Growth, Structural, and Transport Properties of Mn δ-Doped GaAs Layers. *J. Cryst. Growth* **2003**, *251*, 303-310 .

(44) Nazmul, A.M.; Sugahara, S.; Tanaka, M. Transport Properties of Mn δ-Doped GaAs and the Effect of Selective Doping. *Appl. Phys. Lett.* **2002**, *80*, 3120-3122 .

(45) Kawakami, R.K.; Johnston-Halperin, E.; Chen, L.F.; Hanson, Guébels, M. N.; Speck, J.S.; Gssard, A.C.; Awschalom, D.D. (Ga,Mn)As as a Digital Ferromagnetic Heterostructure. *Appl. Phys. Lett.* **2000**, *77*, 2379-2381 .

(46) Kocán, P.; Ohtake, A.; Koguchi, N. Structural Features of Ga-Rich GaAs(001) Surfaces: Scanning Tunneling Microscopy Study. *Phys. Rev. B* **2004**, *70*, 201303(R) .

(47) Ohtake, A. Structure and Composition of Ga-Rich (6×6) Reconstructions on GaAs(001). *Phys. Rev. B* **2007**, *75*, 153302 .

(48) Lee, S.H.; Moritz, W.; Scheffler, M. GaAs(001) Surface under Conditions of Low As Pressure: Evidence for a Novel Surface Geometry*Phys. Rev. Lett.* **2000**, *85*, 3890-3893 .

(49) Kumpf, C.; Marks, L.D.; Ellis, D.; Smilgies, D.; Landemark, E.; Nielsen, M.; Feidenhans'l, R.; Zegenhagen, J.; Bunk, O.; Zeysing, J.H.; Su, Y.; Johnson, R.L. Subsurface Dimerization in III-V Semiconductor (001) Surfaces. *Phys. Rev. Lett.* **2001**, *86*, 3586-3589 .

(50) Ohtake, A.; Kocán, P.; Seino, K.; Schmidt, W.G.; Koguchi, N. Ga-Rich Limit of Surface Reconstructions on GaAs(001): Atomic Structure of the (4×6) Phase. *Phys. Rev. Lett.* **2004**, *93*, 266101 .

(51) Paget, D.; Garreau, Y.; Sauvage, M.; Chiaradia, P.; Pinchaux, R. Schmidt, W.G. X-Ray Diffraction Analysis of the Gallium-Rich Surface of GaAs(001). *Phys. Rev. B* **2001**, *64*, 161305 .

(52) Ohtake, A.; Ozeki, M.; Yasuda, T.; Hanada, T. Atomic Structures of the GaAs(001)-(2×4) Surfaces under As Fluxes. *Phys. Rev. B* **2002**, *65*, 165315 .

(53) Ohtake, A.; Ozeki, M.; Yasuda, T.; Hanada, T. Erratum: Atomic Structures of the GaAs(001)-(2×4) Surfaces under As Fluxes. *Phys. Rev. B* **2002** *66*, 209902 .

(54) Wassermeier, M.; Bressler-Hill, V.; Maboudian, R.; Pond, K.; Wang, X.-S.; Weinberg, W.H.; Petroff, P.M. Scanning Tunneling Microscopy of the Filled and Empty Arsenic States on the GaAs(001)-(2×4) Surface. *Surf. Sci.* **1992**, *278*, L147-L151

Graphical TOC Entry